

NOTE

The Fate of Two SYK-4 Under a Bilinear Coupling

Ruihua Fan^{a,b}

^a*Department of Physics, Peking University*

^b*Institute for Advanced Study, Tsinghua University*

ABSTRACT: In this note, I will discuss various aspects of a generalized SYK model, which contains two SYK-4 coupled with each other via a bilinear term. It has a well defined conformal limit which gives the zero temperature properties of the system. At extremely high temperature, RG analysis tells us the system is asymptotically free. In the intermediate region, interplay among various parameters can give us a rich phase structure. An emergent phase that is absent in conformal limit is also observed.

Contents

1	The Model	1
2	Two Point Function	2
2.1	Conformal Limit	2
2.2	J=0	4
2.3	General Cases	4
3	Lyapunov Exponent	7
3.1	Conformal Limit	8
3.2	General Cases	8
4	Effective Action and Entropy	10
5	Conclusions	12
A	Details of the Calculation at Conformal Limit	14
A.1	Two Point Function in Imaginary Time	14
A.2	Retarded Green's Function in Frequency Domain	14
A.3	Lyapunov Exponent	15
B	Details of the Effective Action	15
C	Analytical Continuation of Two Point Functions	17
C.1	Spectral Decomposition of Various Two-Point Functions and Their Relation	17
C.2	Dyson Equations for Retarded Green's Functions	18

1 The Model

The Hamiltonian is written as,

$$H = \frac{1}{4!} \sum_{ijkl} J_{ijkl} \chi_i \chi_j \chi_k \chi_l + \frac{1}{4!} \sum_{\alpha\beta\gamma\delta} \tilde{J}_{\alpha\beta\gamma\delta} \psi_\alpha \psi_\beta \psi_\gamma \psi_\delta + i \sum_{j,\alpha} V_{j\alpha} \chi_j \psi_\alpha \quad (1.1)$$

where χ_j and ψ_α are different kinds of Majorana fermions. $1 \leq i \leq N$ and $1 \leq \alpha \leq M$ with $p = M/N$ being a tunable parameter. Their anticommutators obeys the following convention,

$$\{\chi_i, \chi_j\} = \delta_{ij}, \quad \{\psi_\alpha, \psi_\beta\} = \delta_{\alpha\beta} \quad (1.2)$$

J_{ijkl} and $\tilde{J}_{\alpha\beta\gamma\delta}$ are two different disorder fields with zero average value,

$$\overline{J_{ijkl}} = \overline{\tilde{J}_{\alpha\beta\gamma\delta}} = 0, \quad \overline{J_{ijkl}^2} = 3!J^2/N^3, \quad \overline{\tilde{J}_{\alpha\beta\gamma\delta}^2} = 3!J^2/M^3 \quad (1.3)$$

$V_{j\alpha}$ is a random coupling,

$$\overline{V_{j\alpha}} = 0, \quad \overline{V_{j\alpha}^2} = t^2/\sqrt{MN} \quad (1.4)$$

Our main interests lies in the phase structure, which will be settled down with the help of two-point functions and Lyapunov exponent.

2 Two Point Function

The two point functions in imaginary time are defined as,

$$G_\chi(\tau) = \mathcal{T} \langle \chi_i(\tau) \chi_j(0) \rangle_\beta, \quad G_\psi(\tau) = \mathcal{T} \langle \psi_\alpha(\tau) \psi_\beta(\tau) \rangle_\beta \quad (2.1)$$

Under large N approximation, the two point functions satisfy the following Dyson equations,

$$\begin{cases} \Sigma_\chi(\tau) = J^2 G_\chi^3(\tau) + V^2 \sqrt{p} G_\psi(\tau) \\ G_\chi^{-1}(\omega) = -i\omega - \Sigma_\chi(\omega) \end{cases} \quad (2.2)$$

$$\begin{cases} \Sigma_\psi(\tau) = J^2 G_\psi^3(\tau) + V^2 \sqrt{\frac{1}{p}} G_\chi(\tau) \\ G_\psi^{-1}(\omega) = -i\omega - \Sigma_\psi(\omega) \end{cases} \quad (2.3)$$

2.1 Conformal Limit

In the low energy limit ($\beta J \gg 1$ and $\beta t \gg 1$), we could drop the $-i\omega$ in the Dyson Equations. Then there is an emergent conformal symmetry for the two-point function which simplifies our calculation.

By simple argument via scaling dimension, we could see that there are three different fixed points,

$$\begin{aligned} [\chi] &= 1/4, [\psi] = 3/4, \chi^4 \text{ and } \chi\psi \text{ are marginal;} \\ [\chi] &= 3/4, [\psi] = 1/4, \psi^4 \text{ and } \chi\psi \text{ are marginal;} \\ [\chi] &= 1/2, [\psi] = 1/2, \text{ only } \chi\psi \text{ is marginal.} \end{aligned}$$

When $p < 1$, χ occupies a larger part. So it is more likely for it to dominate the system. We use the first fixed point to do calculation,

$$G_\chi(\tau) = \left(\frac{1-p}{4\pi J^2} \right)^{1/4} \frac{\text{sgn}(\tau)}{|\tau|^{1/2}} \quad (2.4)$$

$$G_\psi(\tau) = \frac{\sqrt{p}}{4\pi V^2} \left(\frac{4\pi J^2}{1-p} \right)^{1/4} \frac{\text{sgn}(\tau)}{|\tau|^{3/2}} \quad (2.5)$$

The two point function at finite temperature is related to the result above via a reparametrization. If we want to calculation the spectral function, we have to know the retarded Green's

function¹ which can be obtained by analytical continuation $\tau \rightarrow it^2$,

$$G_\chi^R = \sqrt{2}A\theta(t) \left[\frac{\pi}{\beta \sinh \pi t/\beta} \right]^{1/2} \quad (2.6)$$

$$G_\psi^R = -\sqrt{2}B\theta(t) \left[\frac{\pi}{\beta \sinh \pi t/\beta} \right]^{3/2} \quad (2.7)$$

And we can also analytically calculate the $G^R(\omega)$,

$$G_\chi^R(\omega) = \beta \left(\frac{1-p}{4\pi\beta^2 J^2} \right)^{1/4} \frac{\Gamma(1/4 - \frac{\beta}{2\pi}i\omega)}{\Gamma(3/4 - \frac{\beta}{2\pi}i\omega)} \quad (2.8)$$

$$G_\psi^R(\omega) = \beta \frac{\sqrt{p}}{(\beta V)^2} \left(\frac{4\pi\beta^2 J^2}{1-p} \right)^{1/4} \frac{\Gamma(3/4 - \frac{\beta}{2\pi}i\omega)}{\Gamma(1/4 - \frac{\beta}{2\pi}i\omega)} \quad (2.9)$$

Fig 1(a) shows the spectral functions at a typical choice of parameters. The divergence of $A_\psi(\omega)$ at large ω is just due to our over-simple approximation at the conformal limit. Recalling our zero-temperature results, we may think the spectral function can be well fitted by power-law as shown in Fig 1(b). However, the fit only works in the region $\omega > 1/\beta$. This is because the low-energy is different from zero-temperature. Eqn 2.6, valid in the conformal limit, is a low-energy result. Only when $t \ll \beta^3$, the finite-temperature results can be treated as at zero-temperature where two-point functions have perfect power-law behavior.

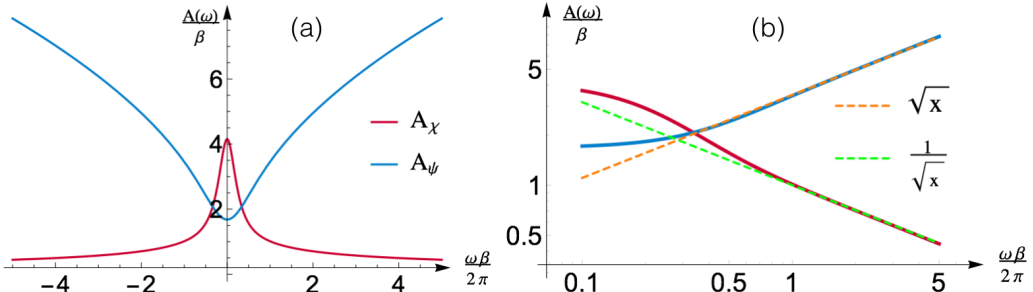


Figure 1. $p = 0.5$, $\beta J = \beta V = 1$. (a) The spectral functions (b) We zoom in a subregion of (a) to get the Figure (b). We use two power-law functions to fit the spectral function. The plot is on a log-log scale. The fit works well after $\omega\beta/2\pi > 1$.

When $p = 1$, the solution above fails so we have to try the last fixed point. And we find that,

$$G_\chi(\tau) = G_\psi(\tau) = \frac{1}{\pi V \tau} + O(1/\tau^3) \quad (2.10)$$

¹Here, the definition of retarded Green's function is $G^R(t) = \theta(t) \langle \{A(t), B(0)\} \rangle_\beta$ which is different from the usual definition(up to a $-i$ factor). Using this definition, the spectral function is defined as,

$$A(\omega) = 2\text{Re } G^R(\omega), \quad G^R(\omega) = \int_0^\infty dt G^R(t) e^{i(\omega+i\epsilon)t}$$

where the extra factor 2 is chosen so that $A(\omega)$ satisfies $\int_{-\infty}^\infty \frac{d\omega}{2\pi} A(\omega) = 1$.

²The continuation schemes for $\tau > 0$ and $\tau < 0$ are different.

³or $\omega \gg \beta$ in frequency domain.

2.2 J=0

When there is only coupling between χ and ψ , the Dyson equations are simplified to quadratic algebraic equations, which gives us two sets of solutions. Using the asymptotic behaviour of $G_\chi(\omega) \rightarrow -1/i\omega$ at large ω , we obtain the physical solution,

$$G_\chi = \frac{\sqrt{p}\omega^2 + (p-1)V^2 - \sqrt{(\sqrt{p}\omega^2 + (1+p)V^2)^2 - 4pV^4}}{2iV^2\omega} \quad (2.11)$$

$$G_\psi = \frac{\sqrt{p}\omega^2 + (1-p)V^2 - \sqrt{(\sqrt{p}\omega^2 + (1+p)V^2)^2 - 4pV^2}}{2ipV^2\omega} \quad (2.12)$$

When $p < 1$, the G_χ around $\omega = 0$ is,

$$G_\chi = \frac{-i\omega}{2\sqrt{p}V^2} \Rightarrow A(\omega = 0) = 0 \quad (2.13)$$

When $p = 1$, the two point functions take simpler forms,

$$G_\chi = \frac{\omega - \sqrt{\omega^2 + 4V^2}}{2iV^2}, \quad G_\psi = \frac{\omega - \sqrt{\omega^2 + 4V^2}}{2iV^2} \quad (2.14)$$

which leads back to the semi-circle law for spectral function.

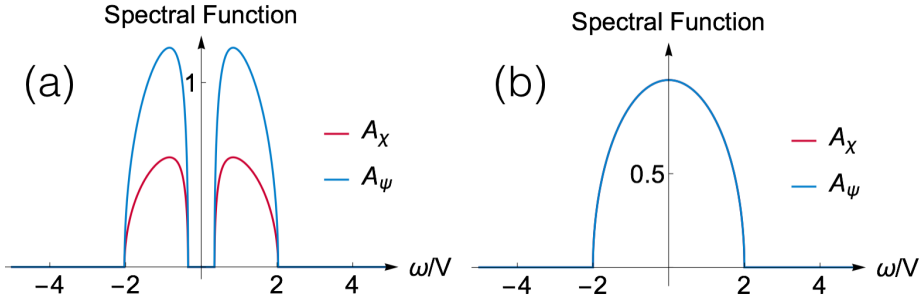


Figure 2. (a) $p = 0.5$ The spectral function show a gap in the low frequency region. (b) $p = 1$ We can clearly see the semi-circle.

2.3 General Cases

For a general choice of parameters, we have to resort to numerics to obtain the two point functions. Fig 3 shows the imaginary-time-ordered Green's functions with typical choices of parameters at conformal limit.

If either βJ or βV is not large enough, there will be numerical result will show large departure from the conformal-limit solution. However, it is a little hard to read the differences between the results at different parameters. So we resort to the spectral function.

If we want to have a look at the spectral function, we have to do analytical continuation of the time-ordered Green's function to get the retarded Green's functions. This can be

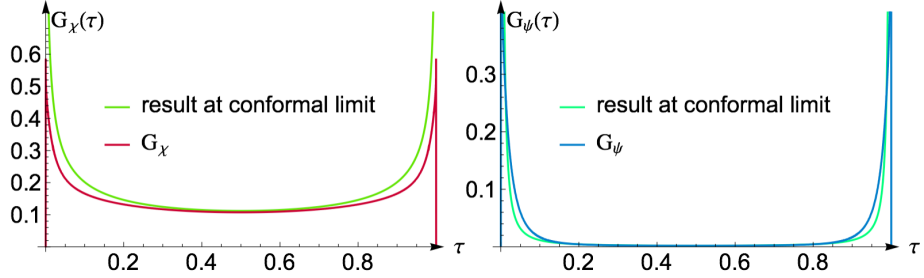


Figure 3. $p = 0.5, \beta J = \beta V = 50$ which is very close to the low-energy regime. So there is only a little discrepancy between the numerical results and the analytical results at conformal limit.

done with either Padé approximation or directly continue the Dyson equations. Here we choose the second method, which is easier in this problem⁴.

The Dyson equation of the retarded Green's function is written as,

$$[iG_\chi^R(\omega)]^{-1} = -\omega - \tilde{\Sigma}_\chi^R(\omega) - it^2\sqrt{p}G_\psi^R(\omega) \quad (2.15)$$

$$[iG_\psi^R(\omega)]^{-1} = -\omega - \tilde{\Sigma}_\psi^R(\omega) - it^2\sqrt{p}G_\chi^R(\omega) \quad (2.16)$$

One can refer to Appendix C.2 for the meaning of the notation.

We first show a result with parameters close to the conformal limit in Fig 4. We could see that for $\omega < \beta$, the numerical results perfectly coincide with the conformal-limit results⁵. For large ω there is no divergence and no discrepancy between the numerics and analytical results.

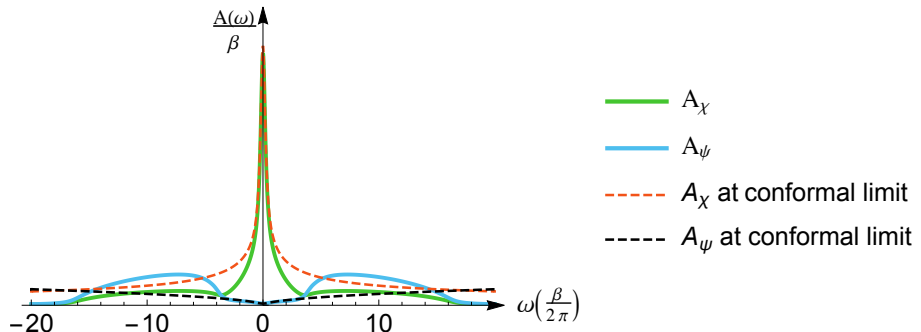


Figure 4. $p = 0.1, \beta J = \beta V = 50$ which is very close to the low-energy regime.

When we tune up the temperature while fixing V/J at a small value, we can see more phases for different $\beta\sqrt{J^2 + V^2}$ and p , some of which are lack at(near) zero temperature.

⁴Padé approximation is a standard method of analytical continuation. Basically it is to use a rational function $P^n(\omega)/Q^m(\omega)$ to approach $\frac{\rho(\omega)}{\omega - z}$. However, in this problem $\rho(\omega) \sim \omega^{-1/2}$ or $\rho(\omega) \sim \omega^{1/2}$ in some regime. So it is hard to use a rational function to simulate such a irrational behavior.

⁵Our RG analysis for the different fixed points valid only when we tune the cutoff down to zero, which is allowed in zero temperature. However, for finite temperature, the cutoff is bounded by the temperature. Only when we consider the physics much smaller than the temperature, can we run the RG down to zero temperature and the analytical analysis valid again. This explains why we can only see the agreement for $\omega < \beta$.

A typical result is shown in Fig 5. The dashed lines means crossover instead of phase transition.

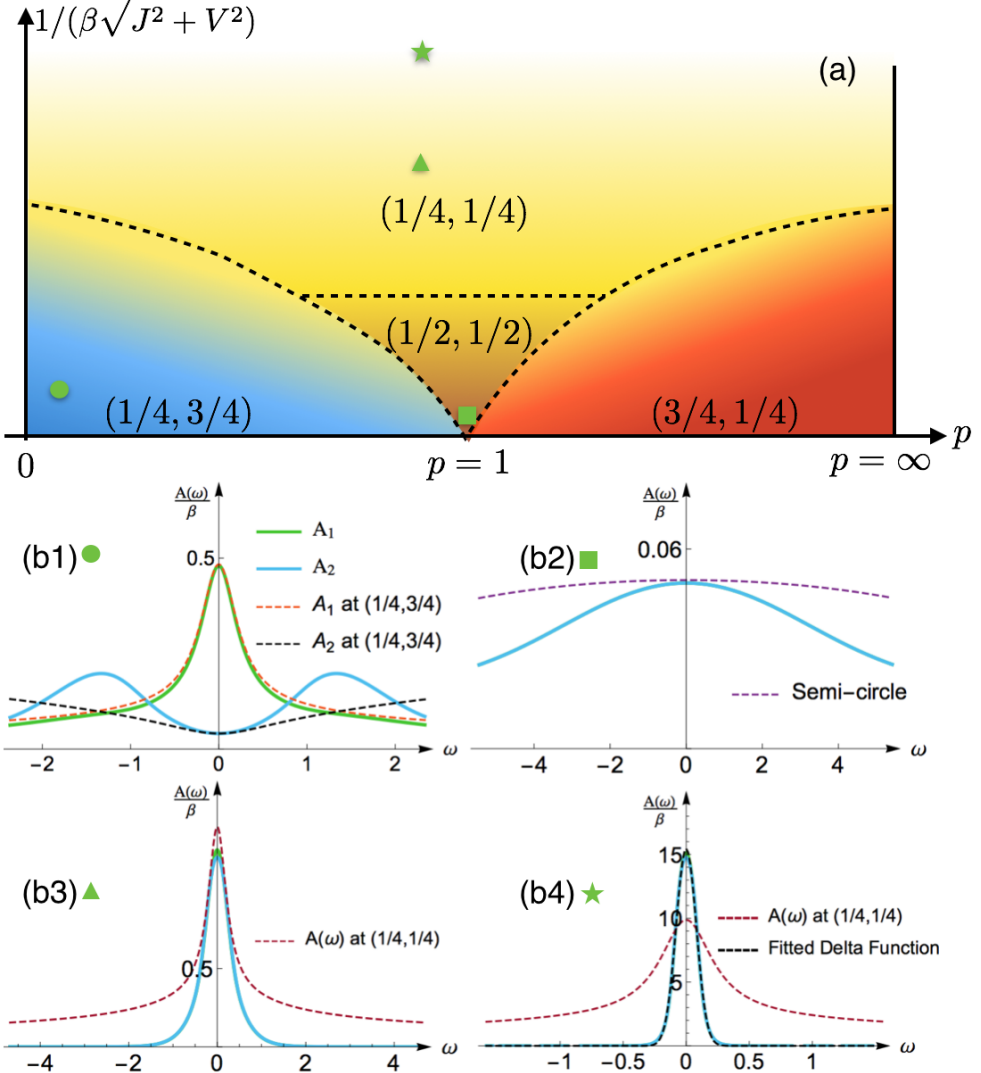


Figure 5. The phase diagram is obtained at $V/J=0.2$, (b1) $p = 0.1$, $\frac{1}{\beta\sqrt{J^2+V^2}} = 0.02$; (b2) $p = 1$, $\frac{1}{\beta\sqrt{J^2+V^2}} = 0.005$; (b3) $p = 0.9$, $\frac{1}{\beta\sqrt{J^2+V^2}} = 0.2$; (b4) $p = 0.9$, $\frac{1}{\beta\sqrt{J^2+V^2}} = 0.9$.

Blue, Red and Brown When the temperature is low enough, the system is well described by the conformal limit and different fields has the corresponding scaling respectively shown on the figure. So if we increase the temperature a bit, it will not have large departure, as indicated by the blue, red and brown regions. We can check the argument by comparing the spectral functions obtained by numerics and analytical method, as shown in Fig 5 (b1) and (b2).

White When the temperature is high enough, which means we are considering high-energy physics, only $\chi\partial_\tau\chi$ and $\psi\partial_\tau\psi$ are relevant. So the system is asymptotically free and we only have many Majorana zero modes. The spectral function is very close to a delta

function sitting at $\omega = 0$ as shown in Fig 5 (b4).

Yellow When the temperature is in a intermediate region, we can numerically solve the spectral functions and compare it with some analytical results, as shown in Fig 5 (b3). We find that A_χ and A_ψ collapse with each other. Both can be well approximated $A(\omega)$ obtained in the low-energy limit of a single SYK-4 model. So we could say both χ and ψ have $1/4$ scaling dimension. This is why we call the yellow region $(1/4, 1/4)$. In zero temperature limit, such a phase only exists when $V/J = 0$. So it is surprising to see this phase emerges at finite temperature for $V/J \neq 0$.

$(1/2, 1/2)$ is a non-chaotic Fermi liquid. $(1/4, 3/4)$, $(3/4, 1/4)$ and $(1/4, 1/4)$ are three chaotic non-Fermi liquid. We will get back to this point and check it by solving the Lyapunov exponent in the following section.

3 Lyapunov Exponent

The Lyapunov exponent is extracted from the exponential deviation behaviour of an OTOC. Here we consider a symmetrized OTOC defined as,

$$F(t_1, t_2) = \text{Tr} \langle W^\dagger(t_1)V^\dagger(0)e^{-\beta H/2}W(t_2)V(0)e^{-\beta H/2} \rangle \quad (3.1)$$

with $t_1 \sim t_2 \gg 0$. In our systems, we have to consider four OTOCs in total,

$$F_{\chi\chi}(t_1, t_2) = \frac{1}{N} \sum_i \langle \chi_i(t_1)\chi_j(0)\chi_i(t_2)\chi_j(0) \rangle \quad (3.2)$$

$$F_{\psi\psi}(t_1, t_2) = \frac{1}{M} \sum_\alpha \langle \psi_\alpha(t_1)\psi_\beta(0)\psi_\alpha(t_2)\psi_\beta(0) \rangle \quad (3.3)$$

$$F_{\chi\psi}(t_1, t_2) = \langle \psi_\alpha(t_1)\chi_j(0)\psi_\alpha(t_2)\chi_j(0) \rangle \quad (3.4)$$

$$F_{\psi\chi}(t_1, t_2) = \langle \chi_j(t_1)\psi_\alpha(0)\chi_j(t_2)\psi_\alpha(0) \rangle \quad (3.5)$$

Each one has a negative disconnected part $-G(t_1 - t_2)G(0) \sim -1$ and a positive disconnected part $\tilde{F}_{\times\times}$ suppressed by a large N factor. The disconnected part will exponentially grow which define the Lyapunov exponent.

The disconnected parts satisfy the following Bethe-Salpeter equations,

$$\begin{pmatrix} \tilde{F}_{\chi\chi} \\ \tilde{F}_{\psi\chi} \end{pmatrix}(t_1, t_2) = \begin{pmatrix} K_{\chi\chi} & K_{\chi\psi} \\ K_{\psi\chi} & K_{\psi\psi} \end{pmatrix}(t_1, t_2; t_3, t_4) \circ \begin{pmatrix} \tilde{F}_{\chi\chi} \\ \tilde{F}_{\psi\chi} \end{pmatrix}(t_3, t_4) \quad (3.6)$$

$$K_{\chi\chi}(t_1, t_2; t_3, t_4) = 3J^2 G_\chi^R(t_{13}) G_\chi^R(t_{24}) G_\chi^{lr}(t_{34})^2$$

$$K_{\chi\psi}(t_1, t_2; t_3, t_4) = V^2 \sqrt{p} G_\chi^R(t_{13}) G_\chi^R(t_{24})$$

$$K_{\psi\psi}(t_1, t_2; t_3, t_4) = 3J^2 G_\psi^R(t_{13}) G_\psi^R(t_{24}) G_\psi^{lr}(t_{34})^2$$

$$K_{\psi\chi}(t_1, t_2; t_3, t_4) = \frac{V^2}{\sqrt{p}} G_\psi^R(t_{13}) G_\psi^R(t_{24})$$

where $G^R(t)$ is real-time retarded Green's function and $G^{lr}(t)$ is Wightman function defined as $G^{lr}(t) = \text{Tr} \langle A(t)e^{-\beta H/2}B(0)e^{-\beta H/2} \rangle$.

3.1 Conformal Limit

If $p = 1$, the system can only stay at the $(1/2, 1/2)$ fixed point. This is a Fermi Liquid, so the Lyapunov exponent is T^2 like.

If $p < 1$, we take the following ansatz,

$$\begin{pmatrix} \tilde{F}_{\chi\chi} \\ \tilde{F}_{\psi\chi} \end{pmatrix}(t_1, t_2) = e^{-h\frac{\pi}{\beta}(t_1+t_2)} \begin{pmatrix} \frac{c_1}{N} \left(\cosh \frac{\pi t_{12}}{\beta} \right)^{h-1/2} \\ \frac{c_2}{\sqrt{MN}} \left(\cosh \frac{\pi t_{12}}{\beta} \right)^{h-3/2} \end{pmatrix} \quad (3.7)$$

The largest $|h|$ satisfies

$$1 = \frac{3 + (-2 - 2h)p^2}{1 - 2h} \quad (3.8)$$

It has $h = -1$ as a p -independent solution, which gives the maximal chaotic behaviour ($\lambda_L = 2\pi/\beta$).

3.2 General Cases

From the symmetry consideration, we can only take $p \leq 1$. We first assume $p < 1$ in the following discussion. And let's consider several limit cases.

We first discuss fixing V/J to be small and tune the temperature from low to high. As we shown in Fig 5, we will go through the $(1/4, 3/4)$, $(1/2, 1/2)$ and $(1/4, 1/4)$ successively and finally fall into a free system. We check this point by solving the spectral function in that section. Now we check this by solving Lyapunov exponent and we will see λ_L will decrease first and increase again followed by a final drop down to zero, as proved in Fig. 6.

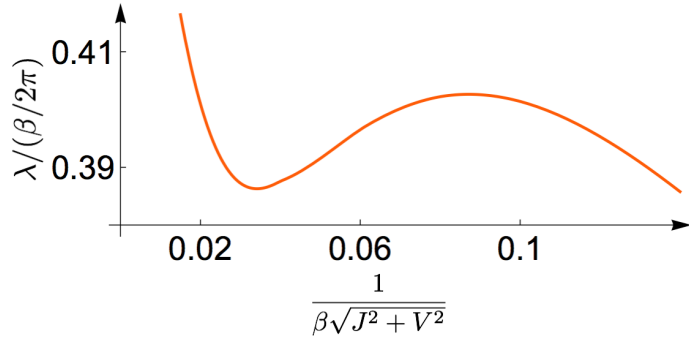


Figure 6. Lyapunov exponent with fixed V/J . The two peaks at low and intermediate temperature means the system is now at a chaotic non-Fermi liquid phase. The first dip means it is at a non-chaotic Fermi-liquid phase. And the final drop means the system gradually become free. $p = 0.6$ and $V/J=0.32$.

The we discuss fixing temperature and tune the coupling V/J .

If the temperature is very high, then the system is asymptotically free, which means the system is non-chaotic at all no matter at what values other parameters are..

If the temperature is very low $\beta\sqrt{J^2 + V^2} \gg 1$. Then we can use the results at conformal limit to make some predictions.

- $V/J \ll 1$, the system is close to two decoupled SYK-4 which will sit near the $(1/4, 1/4)$ fixed point. So the Lyapunov exponent will be close to $2\pi/\beta$ (depends on how low the temperature is).
- As V/J , the system will be driven to the $(1/4, 3/4)$ fixed point, where the Lyapunov exponent will again be close to $2\pi/\beta$. In between, it is hard to make prediction whether the λ_L is large or small.
- $V/J \gg 1$, the fermion bilinear term will eventually dominate, and make the system look like a simple Fermi liquid (corresponds to the $(1/2, 1/2)$ fixed point). So the Lyapunov exponent will be small in this limit.

In Fig 7 we show the numerical results obtained by numerically solving the self-consistent equations of four point functions. Roughly speaking, the decreasing of λ_L means the system is driven away from the $(1/4, 1/4)$ fixed point. And the followed increasing means it is approaching the $(1/4, 3/4)$ region, which indicates the system now again will behaves like a non-Fermi liquid. The final decreasing tells us that the system is destroyed to be a Fermi liquid.

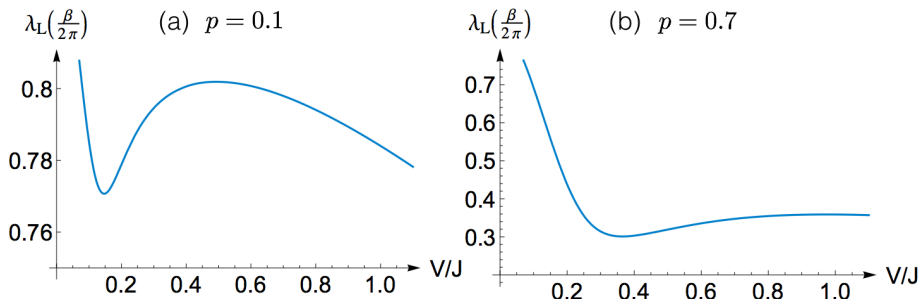


Figure 7. We fix $\beta\sqrt{J^2 + V^2} = 40$. λ_L will decrease first and increase then. When V is large enough, λ_L will decrease to zero.

An exception is of course when $p = 1$. The result in conformal limit tells us the system now at low energy is a Fermi liquid, whose λ_L is much smaller. So after we turn on the coupling, the system will soon be driven away from the $(1/4, 1/4)$ fixed point to the Fermi liquid phase, which is verified in the numerical results of λ_L shown below in Fig 8.

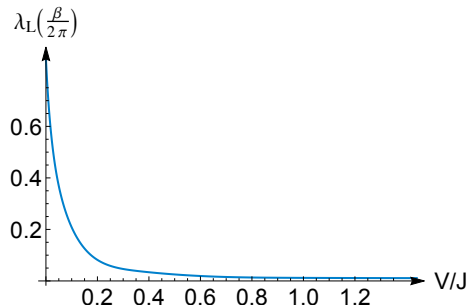


Figure 8. λ_L at $p = 1$, $\beta\sqrt{J^2 + V^2} = 40$. λ_L monotonically decreases with increasing coupling.

What's more, at low temperature, the Lyapunov exponent of a Fermi liquid is proportional to T^2 [2]. So we expect a T^2 at low temperature for the $(1/2, 1/2)$ phase. This can also be directly verified numerically⁶. The result is shown in Fig 9.

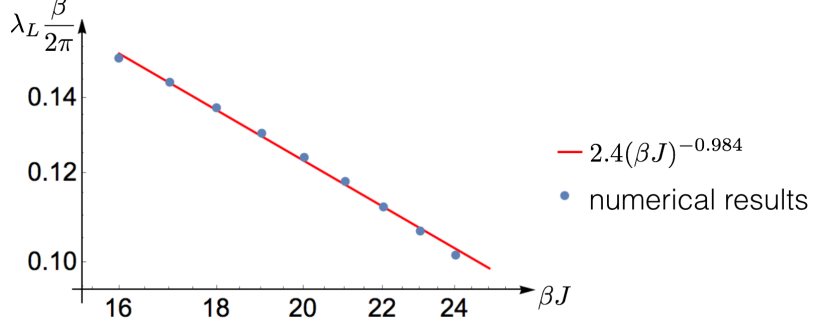


Figure 9. λ_L of the Fermi liquid phase. $p = 1, V/J = 0.5$. The blue dots are numerical data and the red line is fitted curve. The vertical axis is $\lambda_L \beta / 2\pi$ instead of λ_L . And the horizontal axis is βJ instead of T/J . So here slope = -1 means T^2 law.

4 Effective Action and Entropy

To get its effective action using replica trick, we have to assume all the disorder fields obey Gaussian distributions.

$$P(J_{ijkl}) = \frac{1}{\sqrt{2\pi \cdot 3!J^2/N^3}} \exp\left(-\frac{J_{ijkl}^2}{2 \cdot 3!J^2/N^3}\right) \quad (4.1)$$

$$P(\tilde{J}_{\alpha\beta\gamma\delta}) = \frac{1}{\sqrt{2\pi \cdot 3!J^2/M^3}} \exp\left(-\frac{\tilde{J}_{\alpha\beta\gamma\delta}^2}{2 \cdot 3!J^2/M^3}\right) \quad (4.2)$$

$$P(V_{j\alpha}) = \frac{1}{\sqrt{2\pi \cdot V^2/\sqrt{MN}}} \exp\left(-\frac{V_{j\alpha}^2}{2 \cdot V^2/\sqrt{MN}}\right) \quad (4.3)$$

We compute the effective action using replica trick. Perturbatively, the two-point correlation between different replicas is zero. By assuming the preservation of the replica symmetry, we could find that the system is self-average

$$\overline{Z^M} = \overline{Z}^M$$

So that we could deal with \overline{Z} directly. By introducing self-energy and two-point function as two new fields, we can write it as,

$$\overline{Z} = \int D\Sigma D\Gamma \exp(-S_{\text{eff}}) \quad (4.4)$$

⁶In numerics, we have to use a relatively large V/J to avoid the $(1/4, 1/4)$ phase and we cannot go into extremely low temperature for the sake of stability of numerics.

where,

$$\begin{aligned} S_{\text{eff}} = & -N \log Pf(\partial_\tau - \Sigma_\chi) + \frac{\beta}{2} \int d\tau \left(N\Sigma_\chi G_\chi - \frac{NJ^2}{4} G_\chi^4 \right) \\ & - M \log Pf(\partial_\tau - \Sigma_\psi) + \frac{\beta}{2} \int d\tau \left(M\Sigma_\psi G_\psi - \frac{MJ^2}{4} G_\psi^4 \right) \\ & - \frac{\beta}{2} V^2 \sqrt{MN} \int d\tau G_\chi G_\psi \end{aligned}$$

It can be seen clearly that the action has a large N structure which means its saddle point faithfully reflects the system. The classical equations of motion reproduce the Dyson equations encountered at section 2. Taking the saddle point approximation(which is exact under large N), the free energy is directly related to the action.

$$F = -\frac{1}{\beta} \log \overline{Z} = -\frac{1}{\beta} \log \overline{Z} = S_{\text{eff}}/\beta \quad (4.5)$$

In the second equality, we use the fact that the system is self-averaged. As a dimensionless quantity, S_{eff} can only be a function of the dimensionless parameters of the system, say,

$$S_{\text{eff}} = S_{\text{eff}}(\beta J, \beta V, M, N)$$

So we have $\beta \frac{\partial S_{\text{eff}}}{\partial \beta} = J \frac{\partial S_{\text{eff}}}{\partial J} + V \frac{\partial S_{\text{eff}}}{\partial V}$. This can help us to easily obtain the energy,

$$E = \frac{\partial S_{\text{eff}}}{\partial \beta} = - \int_0^\beta d\tau \left(\frac{NJ^2}{4} G_\chi^4 + \frac{MJ^2}{4} G_\psi^4 + V^2 \sqrt{MN} G_\chi G_\psi \right) \quad (4.6)$$

Due to Σ and G obey the equations of motion, the only contribution comes from those terms with explicit dependence of J and t .

The thermodynamic entropy is,

$$\begin{aligned} S = & \log \overline{Z} - \beta \frac{\partial \log \overline{Z}}{\partial \beta} = -S_{\text{eff}} + \beta \frac{\partial S_{\text{eff}}}{\partial \beta} \\ = & N \log Pf(\partial_\tau - \Sigma_\chi) - \frac{\beta}{2} \int d\tau \left(N\Sigma_\chi G_\chi + \frac{NJ^2}{4} G_\chi^4 \right) \\ & M \log Pf(\partial_\tau - \Sigma_\psi) - \frac{\beta}{2} \int d\tau \left(M\Sigma_\psi G_\psi + \frac{MJ^2}{4} G_\psi^4 \right) \\ & - \frac{\beta}{2} V^2 \sqrt{MN} \int d\tau G_\chi G_\psi \end{aligned} \quad (4.7)$$

In the following we consider the entropy density S/N . At very small but still finite temperature,

- When V/J is small, the system behaves like two decoupled SYK-4. So the entropy equals to $(1+p)S_0(\text{SYK}-4)$.

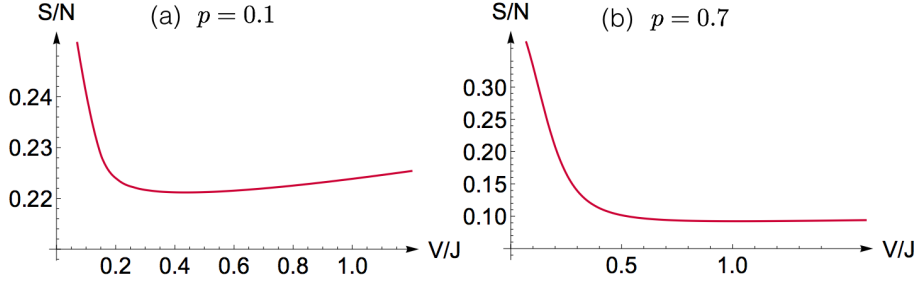


Figure 10. The change of entropy density with respect to coupling V/J . We fix $\beta\sqrt{J^2 + V^2} = 40$. For small p , $|S_{\min} - S_{\max}|$ at zero temperature is large and we can still see the re-increment at a finite temperature. For larger p , say $p = 0.7$ in (b), $|S_{\min} - S_{\max}|$ is small. So curve of S at finite temperature is easily flattened by the temperature.

- When V/J is larger, the system is driven close to the $(1/4, 3/4)$ fixed point. Analytical calculation shows that $S = (1 - p)S_0(\text{SYK} - 4)$.⁷
- After V/J is large enough, the system is close to the $(1/2, 1/2)$ fixed point, which is a fermi liquid. Naive thought will give the prediction of no zero-temperature entropy. However, if, for example, $M < N$, there will be $N - M$ Majorana zero modes surviving the coupling, which gives $(1 - p)\frac{\log 2}{2} > (1 - p)S_0(\text{SYK} - 4)$.

So if we increase βV with $\beta\sqrt{J^2 + V^2}$ fixed, we anticipate the entropy will decrease first followed by a increase at large V/J . This is verified by the numerics shown in Fig 10. For the range shown in Fig 10 (a), the entropy still doesn't have reached $(1 - p)\frac{\log 2}{2}$. But for large enough V/J , it indeed reach the predicted value.

We can see that the variation of entropy is similar to that of Lyapunov exponent shown in Fig 7. To see the comparison more clearly, we plot the entropy and Lyapunov exponent in the same figure shown Fig 11. It is clear that λ_L arrives at the maximum when S/N arrives at the minimum, both are features of the $(1/4, 3/4)$ non-Fermi liquid phase.

5 Conclusions

In spite of the innocuous appearance of a bilinear coupling, such a term brings the system a rich phase structure.

⁷For a single SYK, the conformal limit result tells us that the entropy satisfies,

$$\frac{\partial S}{\partial \Delta} = -\left(\frac{1}{2} - \Delta\right)\pi \tan \pi \Delta$$

By integration, we can see that $S(\Delta = 1/4) = -S(\Delta = 3/4)$.

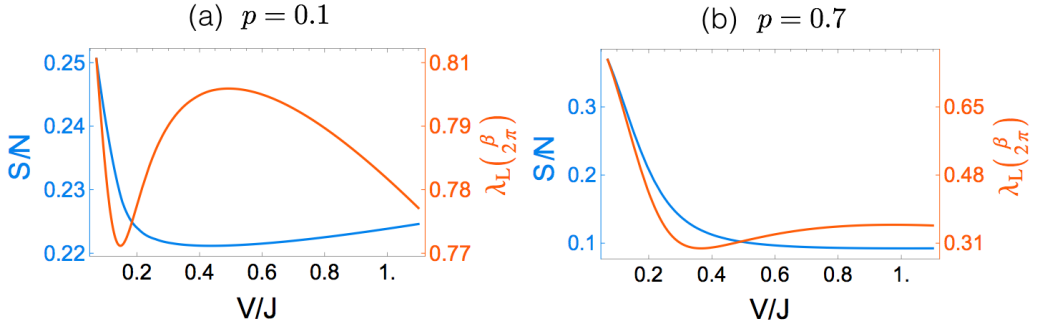


Figure 11. Comparison of entropy and Lyapunov exponent. We fix $\beta\sqrt{J^2 + V^2} = 40$.

Zero Temperature Simply by the RG argument, we could see the system has the following well-defined fixed points, representing different phases,

$$V/J \neq 0 \begin{cases} [\chi] = 1/4, [\psi] = 3/4; \\ [\chi] = 3/4, [\psi] = 1/4; \\ [\chi] = 1/2, [\psi] = 1/2. \end{cases}$$

$$V/J = 0, \quad [\chi] = 1/4, [\psi] = 1/4.$$

$$V/J = \infty, \quad [\chi] = 1/2, [\psi] = 1/2.$$

The scaling above can be made more accurate at the level of two-point function. Analytical calculation shows that $(1/4, 3/4)$ and $(3/4, 1/4)$ phases occur for $p < 1$ and $p > 1$ respectively. And the $V \neq 0$ $(1/2, 1/2)$ phase can only live when $p = 1$. Apart from $(1/2, 1/2)$ phase, all of the other are chaotic non-Fermi liquid and saturate the chaos bound.

Finite temperature All of the zero-temperature phases can still survive at a not very high temperature. What's more, even when V/J is non-zero, the $(1/4, 1/4)$ chaotic non-Fermi liquid can re-occur at the intermediate temperature, which is absent at zero temperature. This is shown in Fig 5.

So if we fix V/J to be small and tune the temperature from low to high, we will go through the $(1/4, 3/4)$, $(1/2, 1/2)$ and $(1/4, 1/4)$ successively and finally fall into a free system.

If we fix $p < 1$, temperature to a low value and tune up V/J from zero, we will go through $(1/4, 1/4)$, $(1/4, 3/4)$ and $(1/2, 1/2)$ respectively.

All of these points can be checked with both spectral function and Lyapunov exponent. When fixing temperature, the thermodynamic entropy is also a useful tool.

Acknowledgments

I'm grateful to my hard-working friends and Prof. Zhai.

A Details of the Calculation at Conformal Limit

A.1 Two Point Function in Imaginary Time

For $p < 1$, we talk the ansatz that,

$$G_\chi(\tau) = a \frac{\text{sgn}(\tau)}{|\tau|^{1/2}}, \quad \tilde{G}_\chi(i\omega) = a 2i\Gamma\left(\frac{1}{2}\right) \sin\left(\frac{\pi}{4}\right) \text{sgn}(\omega) |\omega|^{-1/2} \quad (\text{A.1})$$

$$G_\psi(\tau) = b \frac{\text{sgn}(\tau)}{|\tau|^{3/2}}, \quad \tilde{G}_\psi(i\omega) = b 2i\Gamma\left(-\frac{1}{2}\right) \sin\left(-\frac{\pi}{4}\right) \text{sgn}(\omega) |\omega|^{1/2} \quad (\text{A.2})$$

To solve the Dyson equations, we drop the $J^2 G_\psi^3$ term in Σ_ψ because it is much smaller than G_χ at low energy limit. Then we get,

$$ab = \frac{1}{4\pi V^2} \sqrt{p} \quad (\text{A.3})$$

$$\frac{a^3}{b} = \frac{V^2}{J^2} \left(\frac{1}{\sqrt{p}} - \sqrt{p} \right) \quad (\text{A.4})$$

which gives us the solution.

A.2 Retarded Green's Function in Frequency Domain

We start from a general expression,

$$G^R(t) = A\theta(t) \left[\sinh \frac{\pi t}{\beta} \right]^\alpha = A\theta(t) \left(\frac{e^{\pi t/\beta} - e^{-\pi t/\beta}}{2} \right)^\alpha \quad (\text{A.5})$$

where $\alpha = -2\Delta$ in our case.

$$\begin{aligned} G^R(\omega) &= 2^{-\alpha} A \int_0^\infty dt e^{i\omega t} (e^{\pi t/\beta} - e^{-\pi t/\beta})^\alpha \\ &= 2^{-\alpha} A \int_0^\infty dt e^{i\omega t} e^{\alpha \pi t/\beta} (1 - e^{-2\pi t/\beta})^\alpha \end{aligned}$$

We make a variable substitution $x = e^{-2\pi t/\beta}$. The integral can be written as,

$$G^R(\omega) = 2^{-\alpha} A \frac{\beta}{2\pi} \int_0^1 dx (1-x)^\alpha x^{-\frac{\alpha}{2} - \frac{\beta}{2\pi} i\omega - 1}$$

Recalling the definition of Beta Function $B(p, q) = \int_0^1 dx (1-x)^{p-1} x^{q-1}$, we get the final result,

$$G^R(\omega) = 2^{-\alpha} A \frac{\beta}{2\pi} \frac{\Gamma(\alpha+1)\Gamma(-\frac{\alpha}{2} - \frac{\beta}{2\pi} i\omega)}{\Gamma(\frac{\alpha}{2} - \frac{\beta}{2\pi} i\omega + 1)} \quad (\text{A.6})$$

A.3 Lyapunov Exponent

At conformal limit the retarded Green's functions and Wightman Green's functions can be easily obtained from analytical continuation from the imaginary time results.

For simplicity, we write the ansatz as,

$$\begin{pmatrix} \tilde{F}_{\chi\chi} \\ \tilde{F}_{\psi\chi} \end{pmatrix}(t_1, t_2) = e^{-h\frac{\pi}{\beta}(t_1+t_2)} \begin{pmatrix} c_1/Nf_1(t_{12}) \\ c_2/\sqrt{MN}f_2(t_{12}) \end{pmatrix} \quad (\text{A.7})$$

We drop the $K_{\psi\psi}$ term again because it is much smaller than other terms when consider long time. Notice that $f_2(t) \propto f_1(t)G_\chi^{lr}(t)^2$, the equations can be written as,

$$c_1 e^{-h\frac{\pi}{\beta}(t_1+t_2)} f_1(t_{12}) = (c_1 + \frac{t^2}{3J^2} \frac{\beta}{b^2 \pi} c_2) K_{\chi\chi}(12; 34) \circ e^{-h\frac{\pi}{\beta}(t_3+t_4)} f_1(t_{34}) \quad (\text{A.8})$$

$$c_2 e^{-h\frac{\pi}{\beta}(t_1+t_2)} f_2(t_{12}) = K_{\psi\chi}(12; 34) \circ e^{-h\frac{\pi}{\beta}(t_3+t_4)} c_1 f_1(t_{34}) \quad (\text{A.9})$$

We can make use of the known result (see Section F in ref. [1]) to get the following equations,

$$c_1 = (3J^2 c_1 + t^2 \frac{\beta}{a^2 \pi} c_2) \frac{1}{\tilde{J}_a^2} \frac{1}{1 - 2h} \quad (\text{A.10})$$

$$c_2 = 3b^{2/3} \frac{\pi}{\beta} c_1 t^2 \frac{1}{\tilde{J}_b^2} \quad (\text{A.11})$$

where $\tilde{J}_a^2 = \frac{1}{4\pi a^4}$, $\tilde{J}_b^2 = \frac{1}{4\pi b^{4/3}}$.⁸ Combining them, we could get Eqn (3.8).

B Details of the Effective Action

The replicated partition function under disorder average is (here M is the number of replicas),

$$\begin{aligned} \overline{Z^M} &= \int dJ_{ijkl} d\tilde{J}_{\alpha\beta\gamma\delta} dV_{j\alpha} P(J_{ijkl}) P(J_{\alpha\beta\gamma\delta}) P(V_{j\alpha}) \int D\chi D\psi e^{S^M} \\ &= \int D\chi D\psi \exp(-S^M[\chi] - S^M[\psi] - S^M[\chi, \psi]) \end{aligned} \quad (\text{B.1})$$

where (we use summation over j and α implicitly),

$$S^M[\chi] = \int_0^\beta d\tau \sum_a \frac{1}{2} \chi_j^a \partial_\tau \chi_j^a - \frac{J^2}{8N^3} \int_0^\beta d\tau_1 d\tau_2 \sum_{a,b} (\chi_j^a(\tau_1) \chi_j^b(\tau_2))^4 \quad (\text{B.2})$$

$$S^M[\psi] = \int_0^\beta d\tau \sum_a \frac{1}{2} \psi_\alpha^a \partial_\tau \psi_\alpha^a - \frac{J^2}{8M^3} \int_0^\beta d\tau_1 d\tau_2 \sum_{a,b} (\psi_\alpha^a(\tau_1) \psi_\alpha^b(\tau_2))^4 \quad (\text{B.3})$$

$$S^M[\chi, \psi] = \frac{1}{2} \frac{V^2}{\sqrt{MN}} \int_0^\beta d\tau_1 d\tau_2 \sum_{a,b} \chi_j^a(\tau_1) \psi_\alpha^a(\tau_1) \chi_j^b(\tau_2) \psi_\alpha^b(\tau_2) \quad (\text{B.4})$$

⁸These two auxiliary quantities are defined to utilize the known results.

Because the $\chi\psi - \chi\psi$ scattering process is suppressed by large N , we only make decoupling in $\chi\chi$ and $\psi\psi$ channels.

$$\delta(G_\chi^{ab} - \frac{1}{N}\chi_j^a\chi_j^b) = \int D\Sigma_\chi^{ab} \exp\left(-\frac{N}{2}\Sigma_\chi^{ab}(G_\chi^{ab} - \frac{1}{N}\chi_j^a\chi_j^b)\right)$$

$$\delta(G_\psi^{ab} - \frac{1}{M}\psi_\beta^a\psi_\beta^b) = \int D\Sigma_\psi^{ab} \exp\left(-\frac{M}{2}\Sigma_\psi^{ab}(G_\psi^{ab} - \frac{1}{M}\psi_\beta^a\psi_\beta^b)\right)$$

In terms of G and Σ , the partition function is,

$$\overline{Z^M} = \int D\Sigma DGD\chi D\psi \exp(-S[\chi] - S[\psi] - S[\chi, \psi]) \quad (\text{B.5})$$

where,

$$S[\chi] = \int d\tau_1 d\tau_2 \frac{1}{2} \chi_j^a \left(\delta_{ab} \delta(\tau_1 - \tau_2) \partial_{\tau_2} - \Sigma_\chi^{ab}(\tau_1, \tau_2) \right) \chi_j^b + \frac{N}{2} \Sigma_\chi^{ab} G_\chi^{ab} - \frac{NJ^2}{8} G_\chi^{ab}(\tau_1, \tau_2)^4 \quad (\text{B.6})$$

$$S[\psi] = S[\chi](\chi \rightarrow \psi, N \rightarrow M)$$

$$S[\chi, \psi] = -\frac{V^2}{2} \sqrt{MN} \int d\tau_1 d\tau_2 G_\chi^{ab}(\tau_1, \tau_2) G_\psi^{ab}(\tau_1, \tau_2) \quad (\text{B.7})$$

We assume different replicas don't talk to each other which tells us,

$$\overline{Z^M} = \overline{Z}^M$$

So the system is self-averaged. And we can deal with \overline{Z} directly.

$$\overline{Z} = \int D\Sigma DG \exp(-S_{\text{eff}}) \quad (\text{B.8})$$

where,

$$\begin{aligned} S_{\text{eff}} = & -N \log Pf(\partial_\tau - \Sigma_\chi) + \frac{\beta}{2} \int d\tau \left(N\Sigma_\chi G_\chi - \frac{NJ^2}{4} G_\chi^4 \right) \\ & - M \log Pf(\partial_\tau - \Sigma_\psi) + \frac{\beta}{2} \int d\tau \left(M\Sigma_\psi G_\psi - \frac{MJ^2}{4} G_\psi^4 \right) \\ & - \frac{\beta}{2} V^2 \sqrt{MN} \int d\tau G_\chi G_\psi \end{aligned}$$

And we have used the periodic property of $\Sigma(\tau_1 - \tau_2)$ and $G(\tau_1 - \tau_2)$ to simplify the integration.⁹

⁹ $\int_0^\beta d\tau_1 \int_0^\beta d\tau_2 f(\tau_1 - \tau_2) = \beta \int_0^\beta d\tau f(\tau)$ if the integrand is periodic by shifting β .

C Analytical Continuation of Two Point Functions

C.1 Spectral Decomposition of Various Two-Point Functions and Their Relation

We consider general cases here¹⁰. The retarded Green's function is written as,

$$G^R(t) = \theta(t) \langle \{A(t), B(0)\} \rangle_\beta = \theta(t) \text{Tr} \langle e^{-\beta H} \{A(t), B(0)\} \rangle \quad (\text{C.1})$$

where A and B are two fermionic operators. In terms of the complete set of states, it can be written as,

$$G^R(t) = \theta(t) \sum_{\alpha, \beta} e^{itE_{\alpha\beta}} A_{\alpha\beta} B_{\alpha\beta} (e^{-\beta E_\alpha} + e^{-\beta E_\beta}) \quad (\text{C.2})$$

In frequency domain,

$$G^R(\omega) = \int_{-\infty}^{\infty} dt G^R(t) e^{i(\omega+i\eta)t} = i \sum_{\alpha, \beta} \frac{A_{\alpha\beta} B_{\beta\alpha}}{\omega + E_{\alpha\beta} + i\eta} (e^{-\beta E_\alpha} + e^{-\beta E_\beta}) \quad (\text{C.3})$$

Recalling the formula $\frac{1}{x+i\eta} = P\frac{1}{x} - i\pi\delta(\eta)$, we have,

$$A(\omega) = 2\text{Re}G^R(\omega) = 2\pi \sum_{\alpha, \beta} A_{\alpha\beta} B_{\alpha\beta} (e^{-\beta E_\alpha} + e^{-\beta E_\beta}) \delta(\omega + E_{\alpha\beta}) \quad (\text{C.4})$$

or,

$$A(\omega) = G^R(\omega + i\eta) - G^R(\omega - i\eta) \quad (\text{C.5})$$

Conversely, we could write $G^R(\omega)$ as,

$$G^R(\omega) = i \int \frac{dz}{2\pi} \frac{A(z)}{\omega + i\eta - z} \quad (\text{C.6})$$

We can check that for $A = B = \chi$, we have the following normalization

$$\int \frac{d\omega}{2\pi} A(\omega) = 2.$$

The other two-point function we are interested in can be obtained from $A(\omega)$ via a Hilbert transformation. One is the imaginary-time-ordered Green's function,

$$G(\tau) = \mathcal{T} \langle A(\tau)B \rangle_\beta = \theta(\tau) \text{Tr} \langle e^{-\beta H} A(\tau)B(0) \rangle - \theta(-\tau) \text{Tr} \langle e^{-\beta H} B(0)A(\tau) \rangle \quad (\text{C.7})$$

Using spectral decomposition, we can write it as,

$$G(\tau) = \sum_{\alpha\beta} e^{\tau E_{\alpha\beta}} A_{\alpha\beta} B_{\beta\alpha} (\theta(\tau)e^{-\beta E_\alpha} - \theta(-\tau)e^{-\beta E_\beta}) \quad (\text{C.8})$$

¹⁰For the conciseness of formulas, all the renormalization factor $\frac{1}{Z}$ will be omitted in our following discussion.

In frequency domain,

$$G(i\omega_n) = \int_0^\beta d\tau G(\tau) e^{i\omega_n \tau} = - \sum_{\alpha\beta} \frac{A_{\alpha\beta} B_{\alpha\beta}}{i\omega_n + E_{\alpha\beta}} (e^{-\beta E_\alpha} + e^{-\beta E_\beta}) \quad (\text{C.9})$$

So we have,

$$G(i\omega_n) = - \int_{-\infty}^{\infty} \frac{dz}{2\pi} \frac{A(z)}{i\omega_n - z} \quad (\text{C.10})$$

Comparing with Eqn C.6, we know $G^R(\omega) = -iG(i\omega_n)|_{i\omega_n \rightarrow \omega + i\eta}$.

Another one is the Wightman Green's function,

$$G^{lr}(t) = \text{Tr} \langle e^{-\beta H/2} A(t) e^{-\beta H/2} B(0) \rangle = \sum_{\alpha\beta} e^{-\beta(E_\alpha + E_\beta)/2} e^{iE_{\alpha\beta} t} A_{\alpha\beta} B_{\beta\alpha} \quad (\text{C.11})$$

In frequency domain,

$$G^{lr}(\omega) = \int_{-\infty}^{\infty} dt G^{lr}(t) e^{i\omega t} = 2\pi \sum_{\alpha\beta} e^{-\beta(E_\alpha + E_\beta)/2} A_{\alpha\beta} B_{\beta\alpha} \delta(\omega + E_{\alpha\beta}) \quad (\text{C.12})$$

So we have,

$$G^{lr}(\omega) = \frac{A(\omega)}{\cosh(\beta\omega/2)} \quad (\text{C.13})$$

C.2 Dyson Equations for Retarded Green's Functions

We have known the Dyson equations in imaginary time. Based on the spectral decomposition, we can simply do the analytical continuation $i\omega \rightarrow \omega + i\epsilon$ in frequency domain to get the retarded Green's function. Such a analytical continuation can also be done at the equation level [2].

However, the two first equations of Eqn 2.2 and Eqn 2.3 is written in time domain, which brings us difficulties. So we have to first write down $\Sigma(i\omega_n)$ in terms of spectral functions and do analytical continuation then. For example,

$$\Sigma_\chi(\tau) = J^2 G_\chi(\tau)^3 + t^2 \sqrt{p} G_\psi(\tau) \quad (\text{C.14})$$

The second term is easy to be continued so we only focus on the first term here, written as $\tilde{\Sigma}(\tau)$.

$$\begin{aligned} \tilde{\Sigma}(i\omega_n) &= \int_0^\beta d\tau e^{i\omega_n \tau} \Sigma(\tau) = \frac{J^2}{\beta^2} \sum_{\omega_1, \omega_2} G(i\omega_1) G(i\omega_2) G(i\omega_n - i\omega_1 - i\omega_2) \\ &= \frac{J^2}{\beta^2} \sum_{\omega_1, \omega_2} \int \prod_i \left(\frac{dz_i}{2\pi} A(z_i) \right) \frac{1}{z_1 - i\omega_1} \frac{1}{z_2 - i\omega_2} \frac{1}{z_3 - i\omega_n + i\omega_1 + i\omega_2} \\ &= -J^2 \int \prod_i \left(\frac{dz_i}{2\pi} A(z_i) \right) \frac{n_F(z_1) n_F(z_2) n_F(z_3) + n_F(-z_1) n_F(-z_2) n_F(-z_3)}{i\omega_n - z_1 - z_2 - z_3} \end{aligned}$$

Now we can safely do the replacement $i\omega_n \rightarrow \omega + i\eta$ in the last equation.

$$\begin{aligned}\tilde{\Sigma}^R(\omega) &= -J^2 \int \prod_i \left(\frac{dz_i}{2\pi} A(z_i) \right) \frac{n_F(z_1)n_F(z_2)n_F(z_3) + n_F(-z_1)n_F(-z_2)n_F(-z_3)}{\omega - z_1 - z_2 - z_3 + i\eta} \\ &= iJ^2 \int_{-\infty}^{\infty} dt e^{i(\omega-z_1-z_2-z_3)t} \theta(t) \left[\prod_i \int \frac{dz_i}{2\pi} A(z_i) n_F(z_i) + \prod_i \int \frac{dz_i}{2\pi} A(z_i) n_F(-z_i) \right]\end{aligned}$$

where $n_F(z) = \frac{1}{e^{\beta z} + 1}$ is the Fermi distribution function¹¹. We introduce two auxiliary functions $g(z) = A(z)n_F(z)$ and $\tilde{g}(z) = A(z)n_F(-z)$. So that,

$$\tilde{\Sigma}^R(\omega) = iJ^2 \int_{-\infty}^{\infty} dt e^{i\omega t} \theta(t) (g(t)^3 + \tilde{g}(t)^3) \quad (\text{C.15})$$

And we arrive at the final result,

$$[iG_{\chi}^R(\omega)]^{-1} = -\omega - \tilde{\Sigma}_{\chi}^R(\omega) - it^2 \sqrt{p} G_{\psi}^R(\omega) \quad (\text{C.16})$$

$$[iG_{\psi}^R(\omega)]^{-1} = -\omega - \tilde{\Sigma}_{\psi}^R(\omega) - it^2 \frac{1}{\sqrt{p}} G_{\chi}^R(\omega) \quad (\text{C.17})$$

If we take a more common definition $G^R(t) = -i \langle \{A(t), B(0)\} \rangle_{\beta}$, then we can get rid of the awkward i factors and write the equations as,

$$G_{\chi}^R(\omega)^{-1} = \omega + \tilde{\Sigma}_{\chi}^R(\omega) - t^2 \sqrt{p} G_{\psi}^R(\omega) \quad (\text{C.18})$$

$$G_{\psi}^R(\omega)^{-1} = \omega + \tilde{\Sigma}_{\psi}^R(\omega) - t^2 \frac{1}{\sqrt{p}} G_{\chi}^R(\omega) \quad (\text{C.19})$$

where $A(\omega) = -2\text{Im } G^R(\omega)$ with the definition of $\tilde{\Sigma}(\omega)$ unchanged.

References

- [1] Juan Maldacena and Douglas Stanford, *Remarks on the Sachdev-Ye-Kitaev model*, *Phys. Rev. D* **94** 106002.
- [2] Sumilan Banerjee and Ehud Altman, *Solvable model for a dynamical quantum phase transition from fast to slow scrambling*, arXiv: 1610.04619.

¹¹To get the second equality, we have used the formula $\int_{-\infty}^{\infty} \frac{dt}{2\pi} e^{i\omega t} \theta(t) = \frac{-1}{2\pi i} \frac{1}{\omega + i\eta}$ to replace the $1/(\omega - z_1 - z_2 - z_3 + i\eta)$ with a integral.